한국소음진동공학회 2001년도 춘계학술대회논문집, pp.924~929

2 자유도 Contact Slider 모델의 동특성 해석

0박경수* 전정일** 박영필***

Analysis of Dynamic characteristic of 2-DOF Contact Slider

Kyoung-Su Park, Jeong-Il Chun, and Young-Pil Park

ABSTRACT

The flying height of contact slider is determined by vertical and pitching motions of slider. This paper performed the computer simulation for flying height change of contact slider. It is changed by many parameters, contact stiffness, contact damping, air bearing stiffness ratio, a location of mass center, and so on. Computer simulation is performed for knowing for what change of these parameters influences in flying height of contact slider. Disk surface is modeled in harmonic wave with from 10kHz to 600kHz. Tri-pad slider is modeled in that contact slider has 2-DOF motion (vertical motion, pitching motion). Tri-pad contact slider is analyzed by numerical analysis method in computer simulation.

Keyword : Vertical and pitching motion, Harmonic wave, Contact slider ,Tri pad

1. Introduction

Since 1997, the areal density of magnetic drives has increased from 700 Mb/in^2 to 7 Gb/in^2 in 2000 and is projected to reach 60 Gb/in^2 by the year 2002. And, although magnetic drives will mainly be around 24-36 Gb/in^2 in 2001, a demonstration of 100 Gb/in^2 is expected. The lower flying height is, the higher areal density of magnetic drives increase. But the flying height of present system has approached to several ten nanometer which would be the smallest limit realized for the reduction of the spacing in the flying head system. So the contact head slider/disk interface system is proposed in these days. Because the contact system can have approached to several nanometer flying height, the analysis of dynamic characteristic of contact head slider is important issue in the future magnetic storage devices. The analysis for them was studied with computer simulation by Kyosuke Ono, Takashisa Kato and so on. The Kyosuke Ono analyzed the bouncing vibration of a mono-pad slider with using a single-DOF slider and harmonic wavy surface model [1]. Next, Ono analyzed the bouncing and pitching vibration of tri-pad slider with a two-DOF slider and random wavy surface model [2]. Takahisa Kato and Souta Watarahe develop a computer simulator. They studied the slider motion where a three-DOF model of head-suspension assembly was introduced and the effects of meniscus force due to the meniscus bridge between the slider and the disk was considered[3]. But they scarcely took account of the difference of mass center, operating point of air bearing force, the location of slider and suspension assemble, and so on. They play a very important role to dynamic characteristics of head slider in contact system. In this paper, we study the influences for the change of these parameters with 2-DOF contact slider modeling. Disk surface is modeled in harmonic wave, the frequencies are from 10kHz to 600kHz. Computer analysis is carried out by numerical method, runge-kutta method, also time is done during 4.5 ms, the flying height of contact slider was steadied in 4.3ms ~4.5ms. Through these study, we will know the dominant factors that affects a flying height and dynamic characteristics of contact slider.

* Dep. of Mech. Engineering Yonsei Univ.

** Dep. of Mech. Engineering Yonsei Univ.

*** Prof. Dep. of Mech. Engineering Yonsei Univ.

2. Governing Equation

The tri-pad contact slider used in a numerical analysis has 1.25mm, 1.00mm, 0.3mm (length, width, height). In shown fig.1, the contact slider is modeled two dimensionally. The part of suspension assemble was modeled in bouncing stiffness (k), vertical damping (c), pitching stiffness (k_θ), pitching damping (c_θ). The friction force (μF) operates between contact part of disk surface and slider head. Also the circumference of contact slider pad(1) is 150mm , pad(2) located 153.8mm. Disk

surface is modeled with unit harmonic wavy component,

$$z_d = A\sin(2\pi f_d t - x) \quad (1)$$

When disk spindle rotates at 6000rpm, the air linear velocity through pad(1) has 15m/s and pad(2) has 15.3m/s. The model of contact slider has a static load (F), contact force (F_c), moment (M) and air bearing force that is F_f , F_r . In steady state, when the model has F_0 , M_0 , F_{f0} , F_{r0} . the attitude of contact slider is $z = 0$, $\theta_0 = 300\mu rad$. In this state, if any load and moment add, the equilibrium point of slider is under as δ . In that state, the governing equation for vertical (z_G) and pitching displacement (z_θ) is written as

$$U = (z_G \ , \ z_\theta)$$

$$M\ddot{u} + C\dot{u} + Ku = f_b + f_a + f_c \quad (2)$$

$$M = \begin{bmatrix} m & 0 \\ 0 & j \end{bmatrix}$$

$$C = \begin{bmatrix} c + c_f + c_r & ec + d_f c_f - d_r c \\ ec + d_f c_f - d_r c_r & c_\theta + e^2 c + d_f^2 c_f + d_r^2 c_r \end{bmatrix}$$

$$K = \begin{bmatrix} k + k_f + k_r & ek + d_f k_f - d_r k_r \\ ek + d_f k_f - d_r k_r & k_\theta + e^2 k + d_f^2 k_f + d_r^2 k_r \end{bmatrix}$$

$$f_a = \begin{bmatrix} k_f z_{df} + k_r z_{dr} + c_f \dot{z}_{df} + c_r \dot{z}_{dr} \\ d_r k_f z_{df} - d_r k_r z_{dr} + d_f c_f \dot{z}_{df} - d_r c_r \dot{z}_{dr} \end{bmatrix}$$

$$f_c = \begin{bmatrix} F_c \\ -a_2 F_c - b_2 \mu F_c \end{bmatrix} \qquad f_b = \begin{bmatrix} -F_b \\ -eF_b + M_b \end{bmatrix}$$

Where k_f is air-bearing stiffness at pad(2), k_r is air-bearing stiffness at pad(1). z_{df} and z_{dr} describe the displacement of disk surface. These is described as

$$L_1 = V_1 / f_d \ , \ L_2 = V_2 / f_d$$

$$z_{df} \equiv A\sin(\ 2\pi f_d t - 2\pi(a_2 + d_f)/L_1\ ) \quad (3)$$

$$z_{dr} \equiv A\sin(\ 2\pi f_d t - 2\pi(a_2 - d_r)/L_2\ ) \quad (4)$$

In upper equation,

Contact regime :

$$F_c = 0$$

Non-contact regime :

$$F_c = c_c(\dot{z}_d - \dot{z}_p) + k_c(z_d - z_p) = 0$$

Where z_d describes the displacement of disk surface at slider head part, z_p describes the vertical displacement of slider at head part. The steady state of Equation (2) is $\ddot{u} = \dot{u} = 0$, $z_{df} = z_{dr} = 0$, $\dot{z}_{df} = \dot{z}_{dr} = 0$, $z_G = -\delta$, $z_\theta = 0$, and in these state, the equation for variation is derived,

- Non-Contact state

$$M\ddot{u}^* + C\dot{u}^* + Ku^* = f_a \quad (5)$$

- Contact state

$$M\ddot{u}^* + C^*\dot{u}^* + K^*u^* = f_a + f_c^* \quad (6)$$

Where

$$u^* = \begin{bmatrix} z_G^* \\ \theta^* \end{bmatrix} = u - K^{*-1}f^{-1}$$

$$C^* = C + \begin{bmatrix} c_c & -a_2 c_c \\ -a_2 c_c & a_2^2 c_c \end{bmatrix}$$

$$K^* = K + \begin{bmatrix} k_c & -a_2 k_c \\ -a_2 k_c & a_2^2 k_c \end{bmatrix}$$

$$f^* = \begin{bmatrix} c_c \dot{z}_d & -a_2 k_c \\ -a_2 c_c \dot{z}_d & a_2^2 k_c z_d \end{bmatrix}$$

Where k_c is a contact stiffness. The table 1 and table 2 appear the variable values using simulation. The initial condition of slider is that initial velocity and acceleration are zero in $z_{p0} = 10nm$. The contact slider model that runs between contact regime and non-contact regime is simulated during 4.5ms with a time step of 10^{-9} sec by runge-kutta method.

In this manner, we get the equation of motion for 2-DOF contact slider [4][6].

Table 1. Simulation Parameter Value (Inner)

m	1.6 mg	a_2	0.625 mm
J	$2.19*10^{13}$ kgm^2	b_2	0.15 mm
k	4.9 N/m	d_r	0.125 mm
k_θ	$1.6*10^{-4}$ Nm/rad	d_f	0.5625 mm
ζ	0.002	e	0 ~0.4
ζ_θ	0.002	F	10 mN
ζ_r	0.05	F_{c0}	0.5 mN
ζ_f	0.05	A	$\sqrt{2}$ nm
a	1.25 mm	V_1	15 m/s
b	0.3 mm	V_2	15.3 m/s

Table 2. Simulation Parameter Value (Outer)

Contact stiffness	$k_C = 1.5*10^5$,$1.5*10^6$,$1.5*10^7$
contact damping ratio	$\zeta_C = 0.01$, 0.1
Air bearing stiffness	$k_f = 5.0*10^3$,$5.0*10^4$,$5.0*10^5$
Rear to front air bearing Stiffness ratio	$r = k_r / k_f$ = 0.01 ,0.1 ,10
Coefficient of friction	$\mu = 0.0$

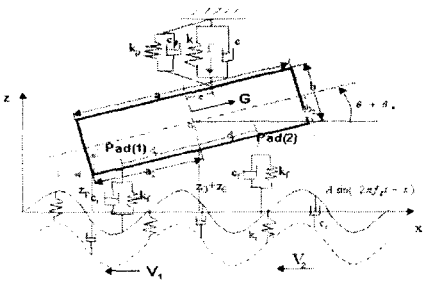

Fig. 1 2-DOF tri-pad contact slider model

3. Simulation result

The dynamic characteristics of slider are gained with through Eq. (5) and Eq. (6) by numerical simulation.

3.1 Characteristics of tri-pad slider

When damping matrix C is zero, we solve Eq. (2) by free vibration analysis. Assume $u^* = Ue^{j\Omega t}$, Eq. (2) is

$$(\Omega^2[M]-[K])\{u\}=0 \tag{7}$$

Multiply $[K]^{-1}$, let $1/\Omega^2=\lambda$

$$([K]^{-1}[M]-\lambda[I])\{u\}=0 \tag{8}$$

Eq. (8) is divided by form of $[M]=[R]^T[R]$,

$$([R][K]^{-1}[R]^T-\lambda[I])\{u\}=0 \tag{9}$$

Also, through natural mode is $U_{ni}=[1\ \ U_{ni}]^T$(i=1,2), we get natural modes. Because of the relation of $U_{ni}\theta=z_G$, U_{ni} is equal to node point of slider. Fig. 2, 3 show the natural frequencies and node point due to the change of rear to front air bearing stiffness ratio r. Ratio r is changed from $r=0.01$ to $r=10$.

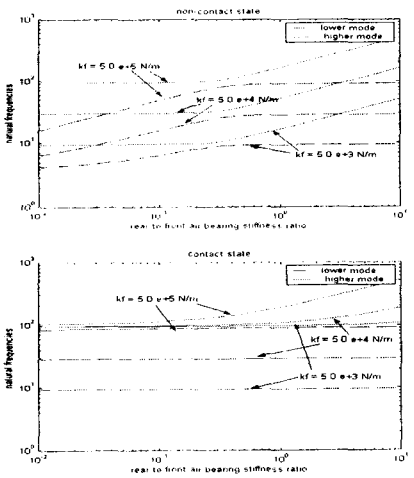

Fig 2 Natural frequencies for air bearing ratio (r)

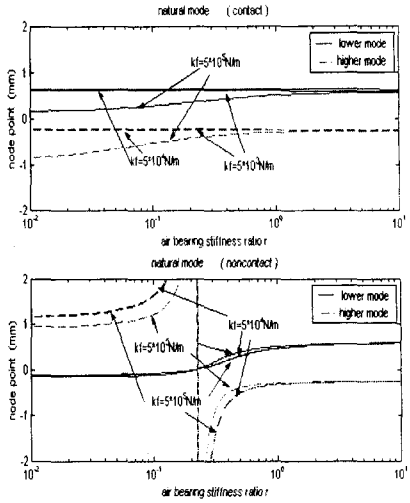

Fig. 3 Natural modes for air bearing ratio (r)

Fig. 2 shows the changes of natural frequency for air-bearing stiffness ratio r. In the case of non-contact, natural frequencies increase when air-bearing stiffness k_f increases. As air-bearing ratio r increases, the gradient of lower mode reduces in the vicinity of r=0.25, the gradient of higher mode increases. As air-bearing ratio r increases, the elements of K_{12}, K_{21} in matrix K changes from the positive to negative in this scope. In the case of contact state, Because k_c has a high value, the elements of K_{12}, K_{21} are the negative in relation of $(ek+d_fk_f-d_rk_r)$. The gradient of lower mode never changes. As shown in the fig. 3, a node point is similar to the change of natural frequencies. But the change of node point has a tendency of opposition with the case of contact. A lower node point locates at trailing edge when k_f is $5.0*10^3$,$5.0*10^4$, does not change. In contact, The change of k_f effects bigger than in non-contact. As air-bearing ratio r gradually increases, the node point of slider converges into trailing edge. It effects the dynamic characteristics of contact slider. Thus air-bearing ratio r plays an important role in dynamic characteristics of contact slider.

3.2 Lift characteristics of contact slider

Fig. 4 shows the lift characteristics of contact slider. Disk surface wave changes from 10kHz to 600kHz with the step of 10kHz. And air-bearing ratio r has the values of 0.01, 0.1, 10. Air-bearing stiffness and contact stiffness change the value of $k_f=5.0*10^3$, $k_f=5.0*10^4$, $k_f=5.0*10^5\ N/m$ and $k_c=1.5*10^5$, $k_c=1.5*10^6$, $k_c=1.5*10^7$ ..Also time varies from 0s to 4.5ms.Natural frequencies of contact slider for these values are written at table 3. When air-bearing ratio r is getting smaller than

0.1, contact slider has a tendency to diverse than to track disk surface. As shown in the fig. 4 (4), (5), (7), (8), (13), (14), (17), (22), (23), (25), (26). When air-bearing ratio r gradually increases, the magnitude of flying height is reduced. When air-bearing ratio r has the level of r=10, the node point of contact slider locates at trailing edge, the head part of slider and air-bearing force operating at trailing edge have bigger value than air-bearing ratio r has small value. In opposite case, when air-bearing force operates the small effect at trailing edge, contact slider does not track disk surface. It appears that the force operating at node point has something to do with the flying height of contact slider. Fig. 4 (a), (b), (c) show the effects of k_f. As k_f increases, the vibration of contact slider reduces, but it is gotten the large effect of resonance. As k_c increases, the amplitude of vibration at trailing edge has a tendency increasing, a strong reflective force operates there. And a strong moment operates at the center of slider. Therefore the flying height of contact slider does not reduce. In the result, for the head part of contact slider has better tracking motion, they should have a big air-bearing stiffness and a small contact stiffness.

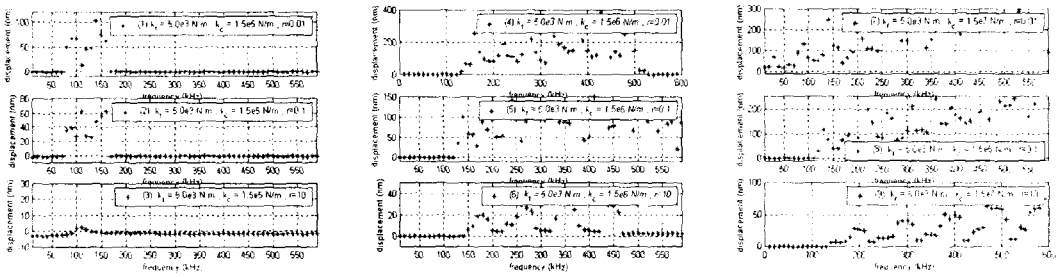

(a) $k_f = 5.0*10^3\ N/m$

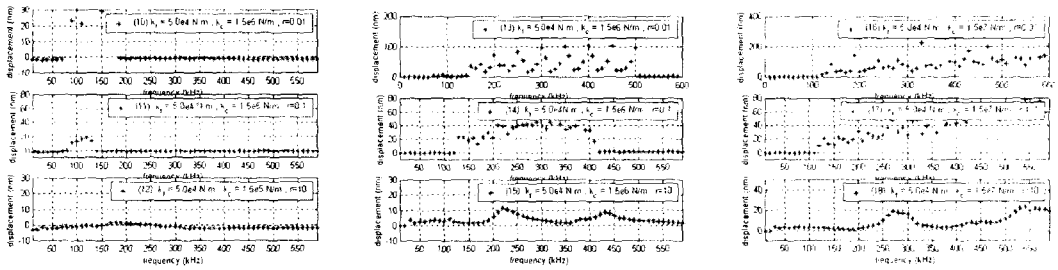

(b) $k_f = 5.0*10^4\ N/m$

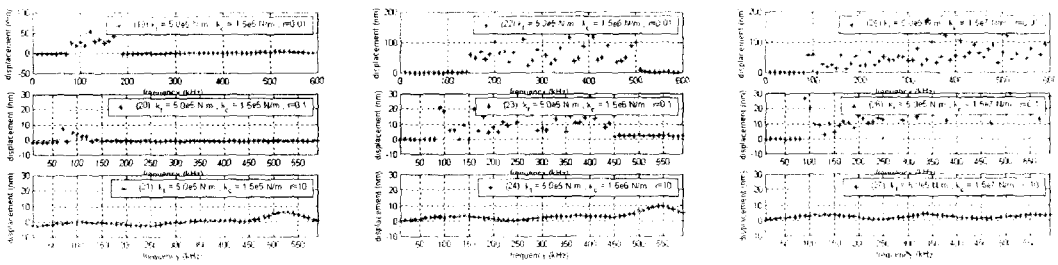

(c) $k_f = 5.0*10^5\ N/m$

Fig. 4 Max height between disk surface and slider head ($\zeta = 0.01$)

Table 3. Natural frequencies for variables (unit : kHz)

	$k_c = 1.5e+5\ N/m$		$k_c = 1.5e+6\ N/m$		$k_c = 1.5e+7\ N/m$	
	r=0.01	r=10	r=0.01	r=10	r=0.01	r=10
5*10³ (N/m)	9.47	9.70	9.47	9.76	9.47	9.77
	95.85	108.66	302.90	307.10	957.45	958.80
5*10⁴ (N/m)	29.14	29.22	29.20	29.91	29.20	30.16
	96.17	188.37	302.90	343.42	957.47	971.05
5*10⁵ (N/m)	84.95	91.12	91.90	92.12	92.09	94.34
	105.35	521.90	303.90	595.57	957.78	1086

3.3 Change of $h_{\max}$ depending on parameters

We choose parameters used in this paper to play an important role in design of slider, suspension and disk.

a) Change of $h_{\max}$ depending on d_r, d_f

We simulate the d_r that is displacement from mass center G of slider to the part of air-bearing force operating at trailing edge effects how $h_{\max}$ changes. In the case of $k_c = 1.5*10^6\ N/m$ and $k_f = 5.0*10^4\ N/m$, fig. 5(a) and fig. 5(b) show the changes of $h_{\max}$ for d_r in $r = 10, d_f$ in $r = 0.01$. As shown in the fig. 5(a), d_r that is a operating point of air-bearing force F_r is dominant factor to determine flying height in $r = 10$. While the flying height due to change of d_f is small. As shown in the fig. 5(b), d_f that air-bearing force F_f operates in is dominant factor to determine flying height in $r = 0.01$. Then the flying height due to change of d_r is small. In $r = 10$, the node point of contact slider locates at the vicinity of trailing edge, so then d_r plays more important role than d_f for the changes of flying height. In contrast with that, the node point of contact slider locates at the vicinity of leading edge, so then d_f plays a important role than d_r for the changes of flying height in r=0.01.

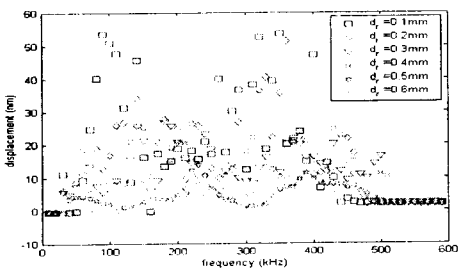

(a)

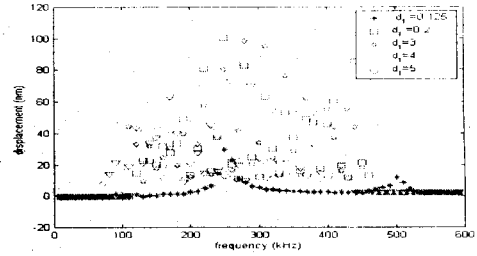

(b)

Fig 5 change of $h_{\max}$ for d_r

b) Change of $h_{\max}$ depending on e

Fig. 6 shows the changes of flying height in condition of $k_f = 5.0*10^5\ N/m$, $k_c = 1.5*10^7\ N/m$, $r = 10$ when the value of e changes into 0.1, 0.2, 0.3 and 0.4. When e goes far apart from mass center, the vibration of contact slier reduces gradually. But $h_{\max}$ increases small at 450kHz. The farther e goes, the lower flying height is. But we are not sure that the slider is stable.

c) Change of $h_{\max}$ depending on mass center

The location of mass center is changeable due to ABS pattern and pad, and so on. So we studied for change of this one in the case of $k_f = 5.0*10^5\ N/m$, $k_c = 1.5*10^6\ N/m$, $r = 10$. When it goes for leading edge, the location of mass center is positive, and it is negative when it goes for trailing edge. As shown in the fig. 7, when e has –0.05, the changes of flying height have a important result. Then they have not the any influence of resonance to 550kHz than when they have other values. Namely, the case is independent on the effect of resonance. Therefore the changes of mass center are also important factor to determine the flying height of contact slider.

d) Change of $h_{\max}$ depending on disk velocity

HDD used in present has the rotating velocity of 10000rpm. So fig. 8 shows the effect of this parameter in $k_c = 1.5*10^6\ N/m$, $k_f = 5.0*10^4\ N/m$, $r = 10$.

In this case, when disk spindle velocity is $V = 15m/s$, the vibration of contact slider reduces in the vicinity of 240kHz due to disk surface wave and $a_2 - d_r = 0.0625mm$ that is displacement between contact point and the operation point of air-bearing force F_r. Also as the velocity increases, the frequency changes into 288kHz, 336kHz, 384kHz for 7200rpm, 8400rpm, 9600rpm. The frequency due to disk surface wave shifts right in frequency domain when the velocity increase.

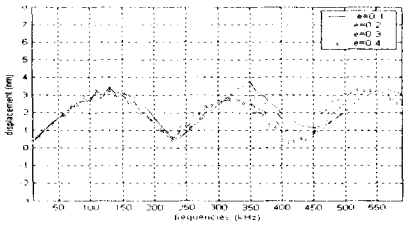

Fig. 6 Change of h_{max} for e

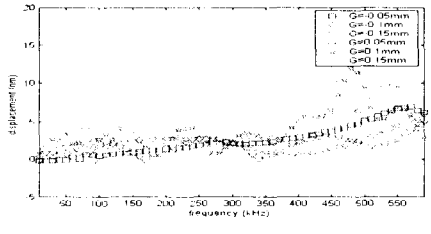

Fig. 7 Change of h_{max} for a mass center

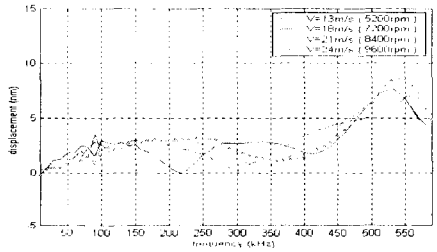

Fig. 8 Change of h_{max} for V

4. Conclusion

(1) The air-bearing stiffness should be small for reducing the vibration of contact slider and being generated the lift characteristics in small scope of frequency domain.

(2) If the node point of lower mode locates at the vicinity of trailing edge, the vibration of low mode is reduced. For that, air-bearing stiffness ratio (r) should get big value.

(3) For the reduction of vibration and the effect of resonance, we should consider the value of parameters, such as d_r , d_f , the bonding point of slider and suspension, the location of mass center, velocity of spindle motor, and so on.

5. Reference

[1]. Kyosuke Ono, Hiroshi Yamamura and Takaki Mizokoshi, 1995, "Computer analysis of the dynamic behavior and tracking characteristics of a single-degree of freedom slider model for a contact recording head", Journal of tribology, Vol 117, pp. 124~129.

[2]. Kan Takahashi and Kyosuke One , 1999 , "Analysis of the bouncing vibrations of a 2-DOF model for tri-pad contact slider with air bearing pads over a harmonic wavy disk surface" , 일본기계학회논문집(C편) 65권 632호, pp.1778~1786.

[3]. Takahisa Kato and Douta Watanabe, Hiroshige Matsuoka, 2001, "Dynamic characteristics of an in-contact head slider considering meniscus for : part 2-application to the disk with random undulation and design conditions", Journal of tribology, Vol 123, pp.168~174.

[4].Kohei Lida and Kyosuke Ono, 2001, "Analysis of bouncing vibrations of a 2-DOF model of tri-pad contact slider over a random wavy disk surface" , Journal of tribology, Vol 123 , pp.159~167.

[5].Ryuuji Tsuchiyama , 1998 , "simulation of dynamics characteristics of head disk interface subjected to wavy excitation and collision in contact magnetic recording" , 일본기계학회논문집(C편) 64권 538호, pp.4791~4797.

[6].Kyouske Ono and Kan Takahashi, 1997, "computer analysis of bouncing vibration and tracking characteristics of a single-degree-of-freedom contact slider model over a random disk surface" , 일본기계학회논문집(C편) 63권 612호, pp.2635~2642 .